Optical properties of Nd^{3+} in Nd_2BaZnO_5

B. Dareys, P. Thurian,* M. Dietrich, M. V. Abrashev,† A. P. Litvinchuk, and C. Thomsen
Institut für Festkörperphysik, Technische Universität Berlin, Hardenbergstraße 36, 10623 Berlin, Germany

A. de Andrés and S. Taboada
Instituto de Cienca de Materiales de Madrid, Consejo Superior de Investigaciones Cientificas, Campus de Cantoblanco, 28049 Madrid, Spain

(Received 9 September 1996)

We present an optical investigation of the crystal-field levels of the Nd^{3+} ion in Nd_2BaZnO_5 by a variety of different optical spectroscopic techniques. The complete fine structure of the first multiplets from $^4I_{9/2}$ to $^4F_{3/2}$ was identified using temperature-dependent photoluminescence and far-infrared reflectivity measurements. In addition, absorption measurements, photoluminescence excitation experiments, and photoluminescence self-absorption were used in order to assign levels up to 28 000 cm^{-1}. The results obtained with independent methods and on different samples are self-consistent. Additional luminescence and absorption lines in the spectra tentatively indicate two different Nd^{3+} sites. A comparison with Nd_2BaCuO_5 is also presented. [S0163-1829(97)01211-3]

INTRODUCTION

R_2BaZnO_5 (R denotes a rare-earth element) crystallizes in two different structures depending on the rare-earth ionic radius. One of them, R_2BaZnO_5 (R denotes Sm, Eu, . . . Tm, Y), is orthorhombic with space group $Pnma(D_{2h}^{16})$.[1] The second family (R denotes La and Nd) is tetragonal, the space group is $I4/mcm(D_{4h}^{18})$, and $Z=4$.[2,3] The latter structure contains Nd-O layers separated by slabs consisting of isolated ZnO_4 tetrahedral units and Ba atoms between them.

Nd_2BaZnO_5 is an insulator and possesses a faint three-dimensional antiferromagnetism up to a Néel temperature of $T_N=40$ K.[4] No other phase transitions are observed up to room temperature. Some of the optical properties of this material have already been studied: the Raman phonons were investigated in Ref. 5, light absorption was reported in Ref. 6 but only in the visible and UV range, and no published luminescence data have become available yet.

For energies greater than $\sim$1000 cm^{-1}, the interaction of Nd_2BaZnO_5 with light is dominated by three electrons of the $4f$ shell of the Nd^{3+} ions. The spectral features related to rare-earth ions in crystals are mainly due to electronic transitions. These may be classified into electric-dipole, magnetic-dipole, and electric-quadrupole transitions.[7] The electric-dipole contribution in spectra is much larger than that of the others and is sufficient to interpret most of spectra.[8] Within the $4f$ shell these transitions are allowed if the surroundings of the ion are such that the nucleus is not situated at a center of inversion. In our compounds this is the case and, consequently, we see a rich series of transitions. Our samples are polycrystalline and in the experimental configuration the area of the light spot on the sample ($\sim$300 μm) is much larger than the typical grain size ($\sim$10 μm); therefore, it is possible to observe all symmetry-allowed transitions.

The first coordination sphere of each Nd ion is formed by eight oxygen ions, at a distance from 2.30 to 2.64 Å, and in this way a NdO_8 polyhedron is built. The Nd ions experience an electric field with a $mm2(C_{2v})$ symmetry, which is sufficiently low to lift completely the degeneracy of all multiplets of the free ion, except for the spin degeneracy. We expect hence a maximum of $(2J+1)/2$ crystal-field (CF) levels per free ion multiplet $^{2S+1}L_J$.

The copper-substituted compound Nd_2BaCuO_5 also exists.[1] In this case, because of the square line shape of the CuO_4 units, the structure crystallizes in the space group $P4/mbm(D_{4h}^5)$. This, however, does not change the site symmetry or the shape of the oxygen environment of Nd in the Nd-O layers. Thus we might expect similar CF levels in both compounds.

The rare-earth-doped single crystals have been investigated extensively as an active medium in lasers,[9] for example, in view of laser-diode pumping applications.[10,11] A good host material should accept a large concentration of optically active rare-earth ions keeping a high radiative rate in comparison to the nonradiative one. The rare-earth ion can occupy several different types of sites having nonequivalent crystal fields, which influences the stimulating properties.[10,12]

In comparison with the doping case, the optical properties of rare-earth ions in the crystallographic cell have been investigated far less. We present here an investigation of the CF levels of Nd^{3+} by means of different optical spectroscopies in two different Nd_2BaZnO_5 samples. A comparison between Zn and Cu compounds is also presented.

EXPERIMENT

We investigated two types of Nd_2BaZnO_5 samples produced independently. They were obtained by solid-state reactions by mixing the starting components (Nd_2O_3, $BaCO_3$, and ZnO) in the appropriate ratio for the nominal content. One of the samples, in the following referred to as A, was calcinated in air at 900 °C for 24 h and then slowly cooled back to room temperature. The resulting powder was pressed into 1-g pellets. The other sample, referred to as B, was also

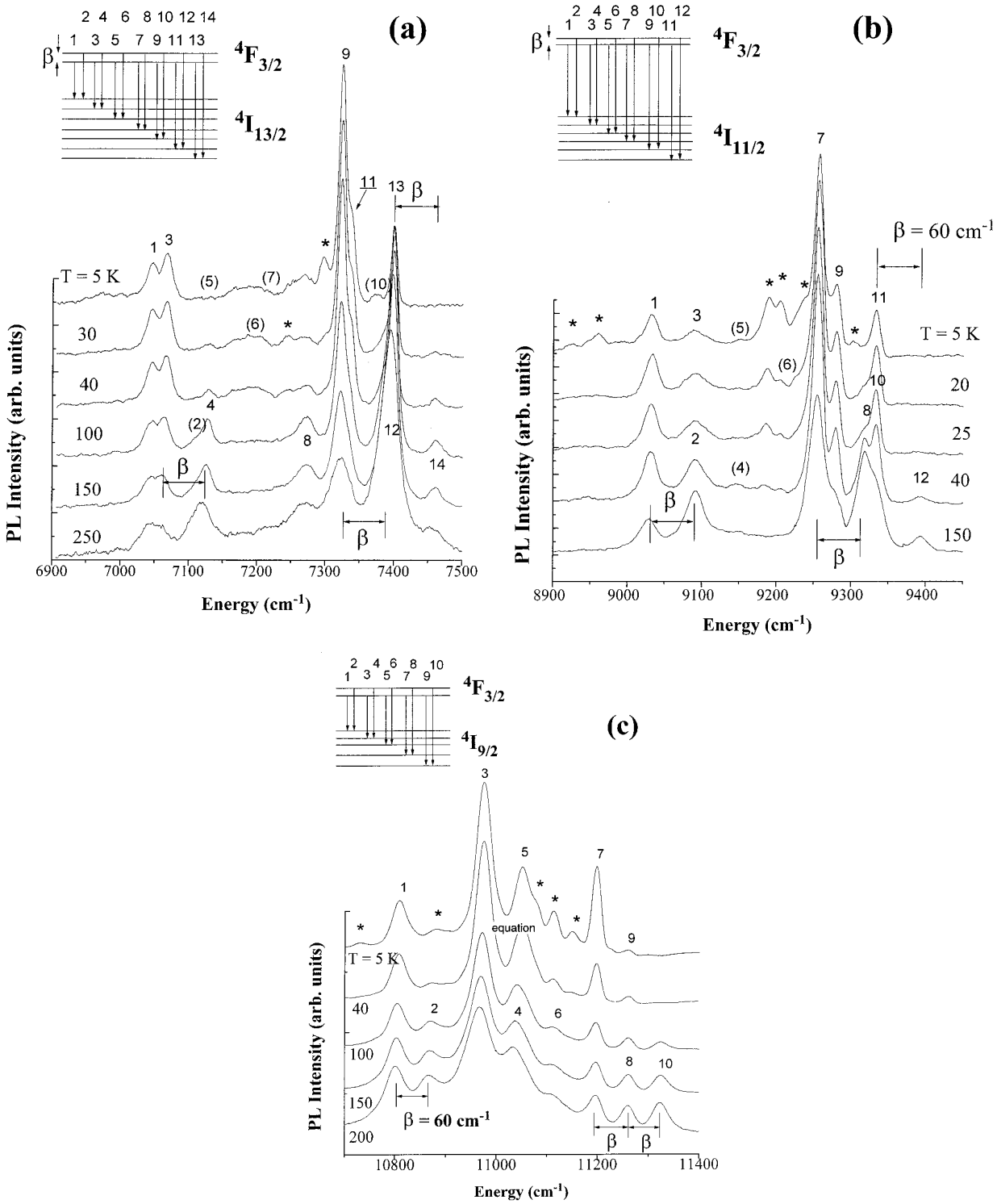

FIG. 1. Photoluminescence spectra of Nd_2BaZnO_5 (sample *A*) for different temperatures from 5 to 250 K. The spectral range corresponds to transitions (a) from $^4F_{3/2}$ to $^4I_{13/2}$, (b) from $^4F_{3/2}$ to $^4I_{11/2}$, and (c) from $^4F_{3/2}$ to $^4I_{9/2}$. The spectra are normalized for the sake of simplicity. The lines marked with an asterisk are not attributed to the Nd ion in the 8(*h*) site of Nd_2BaZnO_5.

calcinated in air at 900 °C for 17 h, but the resulting powder pressed into 1-g pellets was additionally annealed at 1150 °C for several days.

Sample *A* is mat, whitish blue, and because we could separate thin (~200-μm-thick) layers, it was convenient for absorption measurements. Sample *B* is dark brown, was polished with a 1-μm grain diamond paste, and was thus suitably prepared for reflectivity measurements. The synthesis of

TABLE I. Experimental energy levels of Nd^{3+} in Nd_2BaZnO_5. The column labeled ''Measure'' indicates the experiment by which means the energy of the level has been measured (SA denotes self-absorption).

Multiplet	Expt. (cm^{-1})	Calc. (cm^{-1})	Measure	Multiplets	Expt. (cm^{-1})	Calc. (cm^{-1})	Measure
$^4I_{9/2}$	0	−5		$^4F_{9/2}$	14 460	14 461	*A*, SA+PLE
	65	70	All		14 483	14 487	*A*
	216	243	PL		14 516	14 630	*A*, SA
	288	336	PL		14 600	14 684	*A*, SA
	455	493	PL		14 712	14 699	*A*, SA+PLE
$^4I_{11/2}$	1 928	1 916	IR+PL	$^2H_{11/2}$	15 632	15 756	SA+PLE
	1 985	2 026	IR+PL		15 700	15 772	*A*, SA+PLE
	2 007	2 038	IR+PL			15 787	
	2 117	2 148	IR+PL		15 790	15 806	*A*, SA+PLE
	2 170	2 204	IR+PL		15 860	15 820	*A*, SA+PLE
	2 233	2 254	IR+PL		15 890	15 850	*A*, SA+PLE
$^4I_{13/2}$	3 865	3 848	IR+PL	$^4G_{5/2}$	16 540	16 559	*A*, SA+PLE
	3 928	3 973	IR+PL		16 775	16 728	*A*, SA+PLE
	3 942	3 987	IR+PL		16 889	16 913	SA+PLE
	4 050	4 102	IR+PL	$^2G_{7/2}$	16 971	17 027	SA+PLE
	4 133	4 133	IR+PL		17 059	17 076	SA+PLE
	4 200	4 209	IR+PL		17 120	17 143	SA+PLE
	4 220	4 263	IR+PL		17 167	17 191	SA+PLE
$^4I_{15/2}$	5 719	5 779	*A*, IR	$^4G_{7/2}$	18 563	18 533	SA
	5 785	5 911	*A*, IR		18 598	18 591	SA+PLE
	5 840	5 972	*A*, IR		18 643	18 663	SA
	5 896	6 076	*A*, IR		18 897	18 882	SA+PLE
		6 232		$^4G_{9/2}$	18 993	19 025	SA
	6 100	6 310	*A*, IR	$^4K_{13/2}$	19 058	19 111	SA
	6 284	6 366	*A*, IR		19 095	19 154	SA+PLE
	6 361	6 429	*A*, IR		19 168	19 169	SA+PLE
$^4F_{3/2}$	11 263	11 212	PL+*A*+PLE		19 216	19 226	SA
	11 323	11 312	PL+*A*+PLE		19 242	19 244	SA
		12 249			19 272	19 261	SA
$^4F_{5/2}$	12 290	12 272	*A*+PLE			19 314	
	12 385	12 386	*A*+PLE			19 438	
$^2H_{9/2}$		12 428				19 515	
	12 500	12 483	*A*+PLE		19 608	19 616	SA+PLE
		12 545			19 666	19 640	SA
		12 601					
	12 634	12 676	*A*+PLE				
$^4F_{7/2}$	13 220	13 215	SA, *A*+PLE				
	13 260	13 277	SA, *A*+PLE				
	13 376	13 368	SA, *A*+PLE				
		13 420					
$^4S_{3/2}$	13 546	13 513	SA, *A*+PLE				
	13 608	13 518	*A*+PLE				
$^2G_{9/2}$	20 555	20 571	SA+PLE	$^2p_{1/2}$	22 930	22 955	SA+PLE
$^2D_{3/2}$	20 589	20 590	SA	$^2D_{5/2}$	23 202	23 446	SA+PLE
$^4K_{15/2}$	20 631	20 675	SA		23 480	23 495	SA+PLE
$^4G_{11/2}$	20 695	20 693	SA			23 667	

TABLE I. (*Continued*).

Multiplet	Expt. (cm^{-1})	Calc. (cm^{-1})	Measure	Multiplets	Expt. (cm^{-1})	Calc. (cm^{-1})	Measure
	20 777	20 840	SA	$^2P_{3/2}$		25 771	
20 864	20 899	SA+PLE			25 886		
	20 930	20 923	SA	$^4D_{3/2}$		27 084	
		20 967				27 340	
		20 990		$^4D_{5/2}$	~27 570	27 542	PLE
		21 116				27 561	
	21 186	21 181	SA		~28 000	27 749	PLE
		21 233					
		21 293					
		21 297					
		21 396					
		21 429					
		21 483					
		21 498					
		21 534					
		21 607					
	21 650	21 644	SA+PLE				

the Nd_2BaCuO_5 sample was similar to that of sample B.[13] The three samples were characterized using x-ray powder diffractometry, electron microprobe analysis, and Raman microspectroscopy. Within the limits of the accuracy of the methods, the samples appeared to be single phase.

We distinguish two kinds of experiments corresponding to the investigation of luminescence for one part and light absorption for the other. The luminescence was photocreated by the 514-nm line of an Ar-ion laser and detected in the range 6000–28 000 cm^{-1} with a liquid-N_2-cooled Ge photodiode (North Coast EO817L), using a lock-in technique for the IR region, and with a GaAs photomultiplier for the visible region. The light was dispersed in a 0.75-m double-grating monochromator (Spex) 500-nm or 1.6-μm blazed, according to the spectral range involved.

For the absorption investigation, we used different methods depending on the spectral range. From 100 to 7500 cm^{-1} far-infrared reflectivity (FIR) measurements were carried out on a Brucker IFS 66 *V* with the use of triglicine sulfate and HgCdTe detectors and a globar source. The samples were mounted in a He-gas-flow cryostat, allowing variable temperature measurements between 30 and 300 K. The spectral resolution of these measurements was 1 cm^{-1}. From 5500 to 14 000 cm^{-1} the transmittance of light from a halogen lamp through the sample was measured.

At liquid-nitrogen temperature, a broad photoluminescence (PL) was detected [full width at half maximum (FWHM) equal to 3000 cm^{-1}]; it was Gaussian shaped, centered around 16 000 cm^{-1}, and had a few sharp emission peaks. The origin of this broad luminescence is beyond the frame of this work. Between 12 000 and 22 000 cm^{-1} we observed sharp self-absorption lines in the luminescence. The self-absorption effect was observed at helium temperature as well (between 18 600 and 23 500 cm^{-1}), but less clearly so because of the low efficiency of the broad emission band.

Finally, we performed a photoluminescence excitation (PLE) experiment. The excitation was obtained with a 60-W xenon lamp dispersed by a 0.3-m double-grating monochromator, which covered a broad range extending from 10 000 to 28 000 cm^{-1}. The light was dispersed in the micrometer range by a double-prism monochromator (Zeiss MM12).

All spectra were corrected for the respective apparative response. An immersion cryostat was of general use when the temperature of the sample was fixed (1.7, 77, and 300 K). A cold-finger cryostat (Oxford Instruments) was employed for temperature-dependent measurements.

The main part of this work deals with results obtained with sample *A*. We will first discuss the transitions related to $^4F_{3/2}$ to ^4I_J ($2J=9,11,13$) levels and later present results on higher-energy levels. Towards the end, we will present the results concerning sample *B* and the Nd_2BaCuO_5 sample for comparison.

TEMPERATURE-DEPENDENT PHOTOLUMINESCENCE MEASUREMENTS

We begin by discussing the luminescence spectra corresponding to transitions from the $^4F_{3/2}$ doublet to ^4I_J multiplets ($2J=9,11,13$), which dominate the near-infrared spectral region. The respective ranges, which are centered about 11 000, 9200, and 7200 cm^{-1} and are known as normally being free of other transitions, are presented in Figs. 1(a), 1(b), and 1(c), respectively. The photoluminescence was recorded at different temperatures from 5 K to room temperature. The spectral resolution, which amounts at worst to 5 cm^{-1}, is far better than the emission line widths (FWHM of approximately 20 cm^{-1}).

As shown in the inset, we have labeled the transitions thought to arise from the lower $^4F_{3/2}$ level with odd numbers and those from the upper level with even numbers. The transitions originating from the lower $^4F_{3/2}$ level have in common that they are seen down to the lowest temperatures measured. On the other hand, when the temperature increased from 5 to 150 K, the intensity of some lines increased and

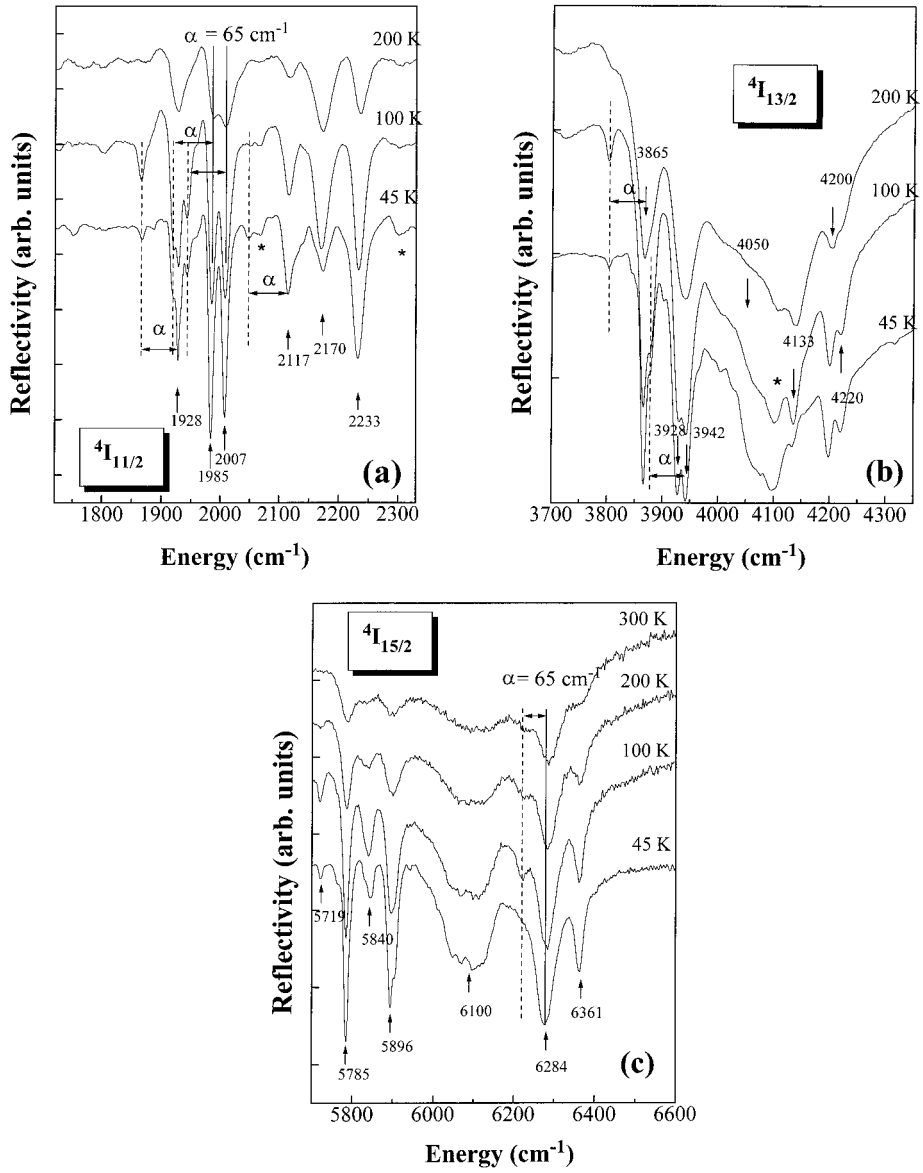

FIG. 2. IR reflectivity spectra of Nd_2BaZnO_5 (sample A) at different temperatures. (a) The lines correspond to absorption from the ground (↑ and full lines) or from the first excited state (dashed lines) of the $^4I_{9/2}$ multiplet into $^4I_{11/2}$. The splitting α between these two states is 65 ± 2 cm^{-1}. (b) The $^4I_{9/2}\rightarrow{}^4I_{13/2}$ transition. A multiplying factor has been applied. The reflectivity is actually smaller than in the $^4I_{11/2}$ range. (c) The $^4I_{9/2}\rightarrow{}^4I_{15/2}$ transition. The multiplying factor is the same as in (b).

some new lines appeared. We attribute these new lines to emission transitions from the upper thermally excited level of the $^4F_{3/2}$ doublet. The temperature dependence occurred mostly below 100 K, as seen in the three spectra recorded at 100, 150, and 250 K in Fig. 1(a) for instance.

In Fig. 1(a) we present the luminescence related to transitions from $^4F_{3/2}$ to $^4I_{13/2}$. The transitions 1, 3, 9, 11 (as a shoulder), and 13 are identified in the spectrum obtained at the lowest temperature (5 K). The even transitions 4, 8, and 14 increase clearly with temperature. We thus determine directly, from the difference in energy of the lines 3 and 4 and of 13 and 14, the splitting of the $^4F_{3/2}$ doublet to be $\beta=60\pm5$ cm^{-1}. Knowing this splitting, we looked for β-split pairs of lines (which are supposed to have the same final state), and thus can thus identify the transitions 2, 7, 10, and 12 by taking the difference to the transitions 1, 8, 9, and 11 in the spectra. Line 6 is positioned from the difference β to line 5, which was seen in absorption. We have thus identified all transitions in the spectra either directly or by taking the difference β between the two $^4F_{3/2}$ levels into account. Lines 4 and 5 are accidently superimposed as well as lines 12 and 13 because two pairs of states of the $^4I_{13/2}$ multiplet have an energy difference similar to the β splitting. Two additional lines labeled with an asterisk at 7250 and 7295 cm^{-1} could not be assigned to the set of transitions of Nd^{3+}. Their intensity is largest at low temperature and they vanish above ~40 K.

The transitions from $^4F_{3/2}$ to $^4I_{11/2}$ and from $^4F_{3/2}$ to $^4I_{9/2}$ were also measured and analyzed in a similar context. In Fig. 1(b) transitions 1, 3, 7, 9, and 11 as well as the even transitions 2, 8, and 12 are clearly identified in the spectra. Lines 4 and 10 are determined by the difference β in the excited state and the pair of lines 5 and 6 is identified by means of FIR reflectivity measurements.

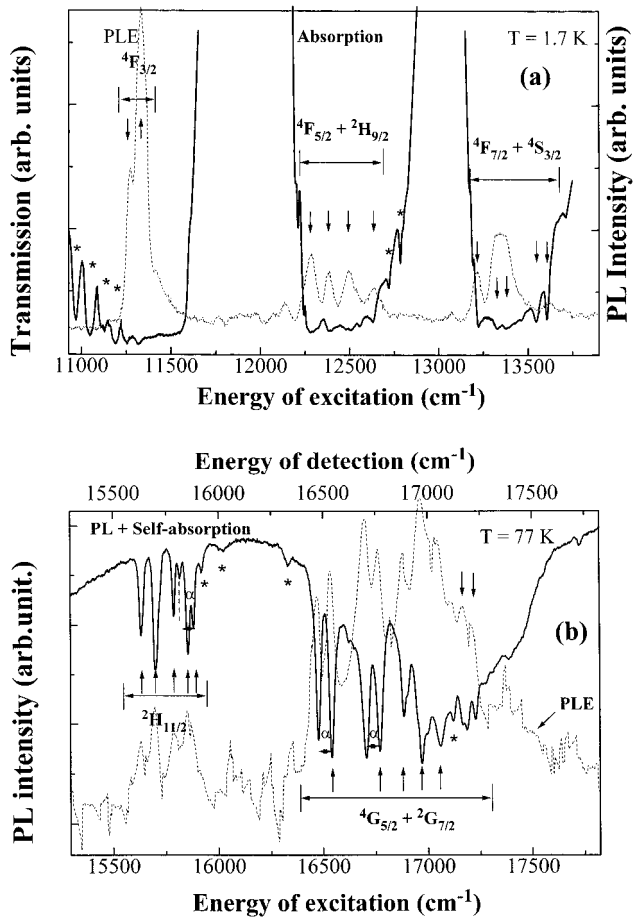

FIG. 3. PLE spectrum (dashed line) of Nd_2BaZnO_5 (sample *A*), for which the detection is set to the $^4F_{3/2} \rightarrow {}^4I_{11/2}$ ($\sim 1\ \mu$m) emission line (bold line). (a) Absorption spectrum in the spectral range corresponding to the $^4F_{3/2}$, $^4F_{5/2}$, $^2H_{9/2}$, $^4F_{7/2}$, and $^4S_{3/2}$ multiplet investigation. (b) PL in the spectral range corresponding to the $^2H_{11/2}$, $^4G_{5/2}$, and $^2G_{7/2}$ multiplet investigation. Three strong absorption lines (α redshifted) are also detected.

In Fig. 1(c) all odd transitions are present on the low-temperature spectrum and conversely the even transitions on the high-temperature one. Lines 9 and 10 are particularly important since they give the absolute energies of the two $^4F_{3/2}$ states. Knowing these values, we were able to work out the absolute energies of all ^4I_J ($2J=9$, 11, and 13) levels from the luminescence data by simple difference; we have compiled them in Table I.

Note the crucial importance of the temperature dependence in the investigation. A systematic quantitative study of the temperature dependence is, however, difficult due to the frequent superposition of lines [see in Fig. 1(a) for instance, the pair (13,14), and the line 12] or their weakness [see also in Fig. 1(a), the pair (7,8)]. The implicit assumption of the temperature independence of the CF levels' position is confirmed by the experiment. The investigation of the $^4I_{15/2}$ multiplet by PL spectroscopy was not possible because we did not have a suitable detector available ($\sim 2\ \mu$m). For higher energies (<800 nm), this method becomes more difficult to use because of the lack of knowledge of the actual multiplets involved.

In the PL spectra, all the observed lines but 13 (7250, 7295, 8924, 8960, 9190, 9205, 9235, 9305, 10 730, 10 882, 11 075, 11 112, and 11 150 cm^{-1}) were successfully assigned to a CF level transition of the Nd^{3+} ion. The additional lines decrease in intensity when the temperature in-

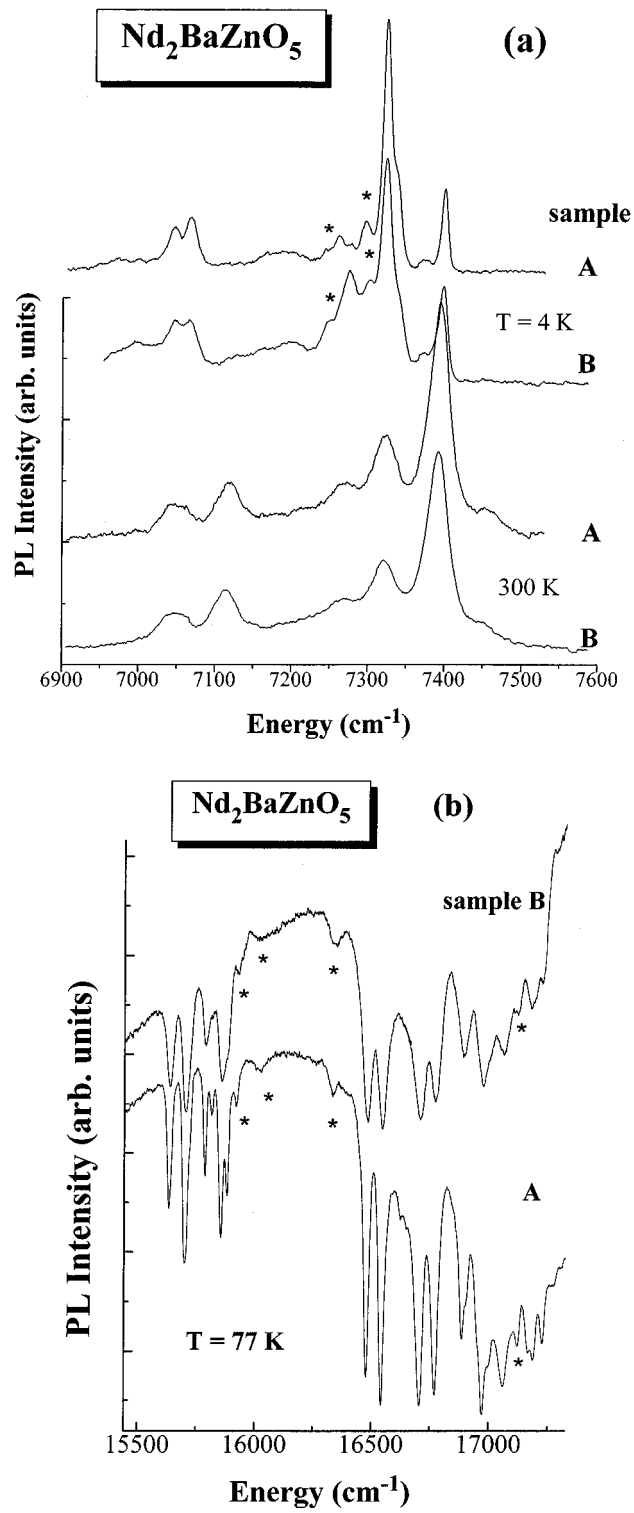

FIG. 4. Comparison of two Nd_2BaZnO_5 samples *A* and *B*. Multiplying and translating factors have been applied for the sake of comparison. (a) PL experiment at 4 and 300 K in the spectral range corresponding to the emission from the $^4F_{3/2}$ to the $^4I_{13/2}$ multiplets. (b) PL experiment at 77 K corresponding to the self-absorption spectral range to the $^2H_{11/2}$, $^4G_{5/2}$, and $^2G_{7/2}$ multiplets.

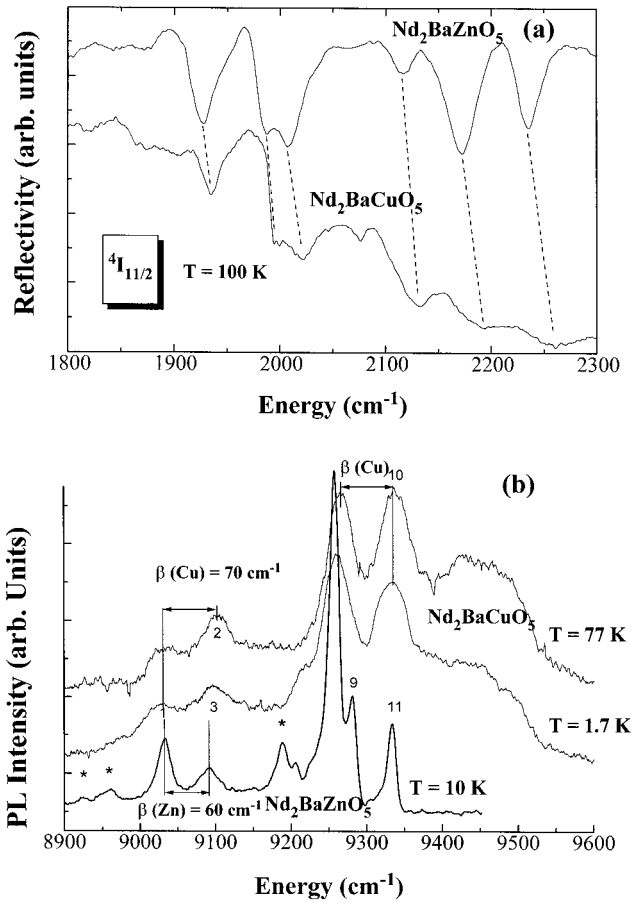

FIG. 5. Comparison of Nd_2BaZnO_5 and Nd_2BaCuO_5 samples. Multiplying and translating factors have been applied for the sake of comparison. (a) FIR reflectivity spectrum at 100 K in the spectral range corresponding to the absorption to the $^4I_{11/2}$ multiplet. (b) PL spectra of Nd_2BaCuO_5 at 1.7 and 77 K and of Nd_2BaZnO_5 at 10 K in the spectral range corresponding to transition from $^4F_{3/2}$ to $^4I_{11/2}$.

creases, disappear above 40 K, and are not necessarily faint. These lines possibly reveal the presence of a second phase; a discussion concerning this point follows towards the end of this paper.

INFRARED REFLECTIVITY MEASUREMENTS ($h\nu$<7000 cm^{-1})

Measurements of the reflectivity were performed in the range between 100 and 7000 cm^{-1} at different temperature from 45 to 300 K. For the main part, the optical index discontinuities are related to interactions either with the lattice vibrations or with the CF levels of Nd, thus allowing an independent confirmation of the PL results described above. Up to 1000 cm^{-1} the CF contribution was overwhelmed by that of the phonons and hence the data did not allow a simple extraction of CF information. The energies of the $^4I_{9/2}$ CF levels thus remain determined by the PL spectroscopy only.

Above 1000 cm^{-1}, after a Kramers-Kronig transformation of the reflectivity spectra to get the absorption, one may directly obtain information about the ground-state transitions from the $^4I_{9/2}$ multiplet to the first few excited multiplets (up to ~7000 cm^{-1}), i.e., to the $^4I_{11/2}$, $^4I_{13/2}$, and $^4I_{15/2}$ multiplets (Table I). Within the accuracy of the measurements, the absorption and reflectivity peak positions are comparable, however. For temperatures where the thermal population of the first excited level of the lowest multiplet $^4I_{9/2}$ was large enough, we could observe absorption originating from this level. Then additional lines appeared in the spectra, redshifted compared to the low-temperature lines by $\alpha=65\pm2$ cm^{-1} (Fig. 2). This shift α, observed seven times, thus corresponds to the splitting between the ground and the first excited state of the $^4I_{9/2}$ multiplet.

The results obtained independently by means of PL and reflectivity measurements on CF levels of the $^4I_{11/2}$ and $^4I_{13/2}$ multiplets were identical except for the 2068-, 2302- [see Fig. 2(a)], and 4100-cm^{-1} [see Fig. 2(b)] lines. These additional lines are probably related to the second phase already observed in the infrared luminescence, although the temperature behavior is different.

TABLE II. Experimental energy levels of Nd^{3+} in Nd_2BaCuO_5.

Multiplet	Energy (cm^{-1})	Measure
$^4I_{11/2}$	1 934	PL, IR
	2 004	PL, IR
	2 021	IR
	2 131	IR
	2 180	PL, ~IR
	2 245	PL, ~IR
$^4I_{13/2}$	3 875	IR
	3 955	IR
$^4F_{3/2}$	11 269	PL
	11 339	PL

ABSORPTION MEASUREMENTS ($h\nu$>11 000 cm^{-1})

We analyze now the data obtained by absorption measurements performed in the visible and near ultraviolet range.

TABLE III. Experimental energy levels of Nd^{3+} in the Ba^{2+} site in Nd_2BaZnO_5. These have been attributed to the additional lines observed in Figs. 1 and 2 (denoted by asterisks).

Multiplet	Energy (cm^{-1})	Measure
$^4I_{9/2}$	0	
	38	PL
	75	PL
	268	PL
	420	PL
$^4I_{11/2}$	1 845	PL
	1 915	PL
	1 945	PL
	1 960	PL
	2 190	PL
	2 226	PL
$^4I_{13/2}$	3 855	PL
	3 900	PL
	4 100	IR
$^4F_{3/2}$	11 150	PL

From a spectral resolution point of view, one can separate our spectra in two parts.

One part consists of photoluminescence excitation experiments at 1.7 K with a resolution of about 90 cm^{-1} (Fig. 3). The detection was set to the emission line of the $^4F_{3/2}$ doublet to either the $^4I_{11/2}$ multiplet (9000 or 9300 cm^{-1}) or the $^4I_{13/2}$ multiplet (7300 cm^{-1}). The spectra were found to be identical, which reflects the similar relaxation of the higher-lying excited states into the $^4F_{3/2}$ states.

The second part is constituted of the light-absorption [Fig. 3(a)] or self-absorption [Fig. 3(b)] experiments with a resolution of typically 1 cm^{-1}. Both measurements together covered a spectral domain from 11 000 to 24 000 cm^{-1}.

Because of the choice of the detection, we obtained two strong lines in the PLE spectrum in the corresponding range of the $^4F_{3/2}$ doublet investigation [see Fig. 3(a)]. The area of the high-energy line relative to the lower one, which reflects the oscillator strength ratio of the two transitions, is about 5. In the absorption spectrum, these two lines also appear at 11 263 and 11 323 cm^{-1}; these energies are of course the same as those of transitions 9 and 10 in the PL spectrum of Fig. 1(c). We thus measured again, more precisely, the splitting of the $^4F_{3/2}$ doublet $\beta=60\pm3$ cm^{-1}.

Note the different but complementary features of the two types of measurements. On the one hand, the absorption measurements are spectrally well resolved but too sensitive (five sharp lines appear in the 11 000–11 500 cm^{-1} range where only two are expected) and, on the other hand, the PLE measurements are selective but the spectral resolution was not satisfactory for a unique assignment.

The low sensitivity of the PLE measurements did not allow the assignment of all the states of the multiplets; see the blanks in Table I. In Fig. 3(b) we present PLE spectra as well as PL spectra with self-absorption transitions in the range 15 000–18 000 cm^{-1}, in which the $^2H_{11/2}$, the $^4G_{5/2}$, and the $^2G_{7/2}$ multiplets are expected. In the spectrum of Fig. 3(b), the spectral resolution of the PLE experiment is better (50 cm^{-1}), but the signal is also noisier. Once more, the PLE lines played the role of an ''indicator'' in the spectrally more resolved absorption data. Because both spectra were recorded at 77 K, three α redshifted absorption lines coming from the first excited state could be observed additionally (at 1.7 K, they are not observed in PLE). The splitting, as above, was found to be $\alpha=65\pm2$ cm^{-1}.

Above 18 000 cm^{-1}, the only data on the CF levels available came from the self-absorption effect and the PLE gave only little information. Since the number of lines observed was smaller than expected, i.e., less $(2J+1)/2$ states per multiplet, all experimental lines were assigned.

Table I gathers all experimental results in the column labeled ''Expt.,'' specifying for each level, in the column ''Measure,'' what kind of experiments had been used. The experimental accuracy is typically ±3 cm^{-1}. The plus sign links two associated experiments and the comma refers to independent determinations. As can be seen, most levels have been determined several times independently, up to five for the first excited state (65 cm^{-1}). We quote, in the column ''Calc.,'' the calculation performed by Taibi *et al.*[6] in the frame of a crystal-field symmetry of C_{2v}. This calculation allows us to predict the position of the states we do not observe (the dash in the ''Expt.'' column).

We repeated all measurements (except for the PLE) on sample *B* in somewhat more restricted spectral ranges. In Fig. 4 PL results in the region of $^4F_{3/2}\rightarrow{}^4I_{13/2}$ transitions obtained from samples *A* and *B* are presented for comparison at two temperatures. The two differently prepared samples gave nearly identical results in luminescence [Fig. 4(a)] and in absorption [Fig. 4(b)], including the observation of the second phase (the asterisks in Fig. 4). The reproducibility of the results for two different Zn samples ensures their reliability and gives us confidence in our assignment to the crystal-field transitions of Nd^{3+}.

COMPARISON BETWEEN Nd_2BaZnO_5 AND Nd_2BaCuO_5 SAMPLES

We performed also IR reflectivity measurements on the Nd_2BaCuO_5 sample. Figure 5(a) presents the spectral range concerning the $^4I_{11/2}$ multiplet. Six features in the Cu-compound spectrum correspond to the six lines of Nd in the Zn compound. They are 1000 times fainter, significantly broader, and blueshifted ($\sim$10–20 cm^{-1}) in the Cu compound, but with the same relative intensities [Fig. 5(a)].

Finally, we recorded the luminescence of the Cu compound, at 1.7 and 77 K, in the spectral range near 9000 cm^{-1}, where the $^4F_{3/2}\rightarrow{}^4I_{11/2}$ emission is expected. As in absorption, the luminescence is much fainter than in the Zn compound, and because the lines are about twice as broad, we distinguish clearly only four. As can be seen in Fig. 5(b), these four lines can be found in the luminescence spectrum of Nd_2BaZnO_5 as well. As in this material, they are connected with emission transitions from the two states of the $^4F_{3/2}$ doublet to two states of the $^4I_{11/2}$ multiplet. In analogy to the transitions in Nd_2BaZnO_5, we thus identify the transitions 1, 3, 9, and 11 in Nd_2BaCuO_5 on the 1.7-K spectrum and the transitions 2 and 10 on the 77-K spectrum. These two last lines increase in intensity with temperature and accidentally overlap the lines 3 and 11, respectively, as it does in the Zn compound. This allows us to determine the splitting of the $^4F_{3/2}$ states of Nd^{3+} states to be $\beta(\mathrm{Cu})=70\pm5$ cm^{-1}. The results of the copper compound are compiled in Table II.

Let us discuss now the possible origin of the second phase. In principle, one can think about a trace of Nd_2O_3, which is a starting compound and could have remained after preparation.[6,14] In order to decide this, we performed reflectivity and PL measurements in the FIR and IR ranges, respectively, on a pulver of this oxide. We found that the optical properties of this oxide had nothing in common with our second phase. Data already compiled in the literature[15] confirmed this assertion. Therefore, Nd_2O_3 is not at the origin of the additional lines observed.

One could argue, on the other hand, that in Nd_2BaZnO_5, Nd^{3+}, in addition to its 8(*h*) site, could be placed on the 4(*a*) site of Ba^{2+}. Either way, our results indicate that optical measurements can be more sensitive to the presence of a second phase or an interchance of Nd and Ba sites than standard x-ray powder patterns.

From the 13 additional luminescence lines, we extract some CF levels of the Nd in the second phase, assuming that

the highest-energy emission line [11 150 cm^{-1} in Fig. 1(c)] is the transition from the lower level of $^4F_{3/2}$ multiplet to the ground state. The results are gathered in Table III.

CONCLUSION

In summary, using a variety of optical techniques, we were able to assign all crystal-field energy levels of the five lowest multiplets of Nd^{3+} in Nd_2BaZnO_5 and many additional levels in the energy range up to 28 000 cm^{-1}. The levels involved go up to $^4D_{5/2}$. The appearance of a second phase in or a hypothetical placement of Nd on a Ba site in Nd_2BaZnO_5 yields a second (partial) set of crystal-field transitions. Finally, we determined the fine structure of the $^4I_{11/12}$ and $^4F_{3/2}$ multiplets in the corresponding Cu compound Nd_2BaCuO_5.

ACKNOWLEDGMENTS

B.D. and A.P.L. have been supported by the European Union under Contract Nos. ERBCHBG-CT93-0240 and ERBCMBI-CT94-1659. M.V.A. acknowledges the financial support from the Alexander von Humboldt Foundation (Bonn, Germany).

*Author to whom correspondence should be addressed. Electronic address: thurian@physik.tu-berlin.de

†Permanent address: Faculty of Physics, Sofia University, BG-1126 Sofia, Bulgaria.

[1] C. Michel and B. Raveau, J. Solid State Chem. **49**, 150 (1983).

[2] C. Michel, L. Er-Rakho, and B. Raveau, J. Solid State Chem. **42**, 176 (1982).

[3] M. Taibi, J. Aride, J. Darriet, A. Moqine, and A. Boukhari, J. Solid State Chem. **86**, 233 (1990).

[4] G. G. Chepurko *et al.*, Phys. Lett. A **157**, 81 (1991).

[5] M. V. Abrashev, G. A. Zlateva, M. N. Iliev, and M. Gyulmezov, Phys. Rev. B **49**, 11 783 (1994); see also E. J. Baran, A. E. Lavat, R. Saez-Puche, and A. Salinas Sanchez, J. Mater. Sci. Lett. **11**, 1087 (1992).

[6] M. Taibi, J. Aride, E. Antic-Fidancev, M. Lemaitre-Blaise, and P. Porcher, Phys. Status Solidi A **115**, 523 (1989).

[7] J. H. Van Vleck, J. Phys. Chem. **41**, 67 (1937).

[8] B. R. Judd, Phys. Rev. **127**, 750 (1962); G. S. Ofelt, J. Chem. Phys. **37**, 511 (1962).

[9] G. D. Gilliland, R. C. Powell, and L. Esterowitz, Phys. Rev. B **38**, 9958 (1988).

[10] M. D. Seltzer, J. B. Gruber, M. E. Hills, G. J. Quarles, and C. A. Morrison, J. Appl. Phys. **74**, 2821 (1993).

[11] G. J. Quarles, L. Esterowitz, G. H. Rosenblatt, M. H. Randles, J. E. Creamer, and R. F. Belt, SPIE Proc. **1627**, 168 (1992).

[12] G. J. Quarles, A. Suchocki, R. C. Powell, and S. Lai, Phys. Rev. B **38**, 9996 (1988).

[13] M. V. Abrashev, G. A. Zlateva, and E. Dinolova, Phys. Rev. B **47**, 8320 (1993).

[14] M. Taibi *et al.*, J. Solid State Chem. **74**, 329 (1988).

[15] P. Caro, J. Derouet, and L. Beaury, J. Chem. Phys. **70**, 2542 (1979).